



King Saud University  
Arabian Journal of Chemistry

www.ksu.edu.sa  
www.sciencedirect.com



## ORIGINAL ARTICLE

# Use of response surface methodology for optimization of fluoride adsorption in an aqueous solution by Brushite

M. Mourabet \*, A. El Rhilassi, H. El Boujaady, M. Bennani-Ziatni, A. Taitai

Team Chemistry and Valorization of Inorganic Phosphates, Department of Chemistry, Faculty of Sciences,  
BP 133, Kenitra 14000, Morocco

Received 16 November 2012; accepted 31 December 2013

## KEYWORDS

Brushite;  
Adsorption;  
Box–Behnken model;  
Desirability function;  
Fluoride

**Abstract** In the present study, Response surface methodology (RSM) was employed for the removal of fluoride on Brushite and the process parameters were optimized. Four important process parameters including initial fluoride concentration (40–50 mg/L), pH (4–11), temperature (10–40 °C) and B dose (0.05–0.15 g) were optimized to obtain the best response of fluoride removal using the statistical Box–Behnken design. The experimental data obtained were analyzed by analysis of variance (ANOVA) and fitted to a second-order polynomial equation using multiple regression analysis. Numerical optimization applying desirability function was used to identify the optimum conditions for maximum removal of fluoride. The optimum conditions were found to be initial concentration = 49.06 mg/L, initial solution pH = 5.36, adsorbent dose = 0.15 g and temperature = 31.96 °C. A confirmatory experiment was performed to evaluate the accuracy of the optimization procedure and maximum fluoride removal of 88.78% was achieved under the optimized conditions. Several error analysis equations were used to measure the goodness-of-fit. Kinetic studies showed that the adsorption followed a pseudo-second order reaction. The equilibrium data were analyzed using Langmuir, Freundlich, and Sips isotherm models at different temperatures. The Langmuir model was found to be describing the data. The adsorption capacity from the Langmuir isotherm ( $Q_L$ ) was found to be 29.212, 35.952 and 36.260 mg/g at 298, 303, and 313 K respectively.

© 2014 King Saud University. Production and hosting by Elsevier B.V. All rights reserved.

## 1. Introduction

Fluoride can cause significant effects in humans through drinking water. At low concentrations, it has beneficial effects on teeth and bones. However, excessive intake of fluoride provokes skeletal fluorosis, which is associated with serious bone. The World Health Organization has specified the tolerance limit of fluoride content of drinking water as 1.5 mg/L (WHO, 2006). Hence, an excess amount of fluoride in drinking water must be removed using appropriate technologies. To reduce fluoride concentration in naturally high fluoride waters

\* Corresponding author. Tel.: +212 618494233.  
E-mail address: [mrab.et@hotmail.com](mailto:mrab.et@hotmail.com) (M. Mourabet).  
Peer review under responsibility of King Saud University.



Production and hosting by Elsevier

or fluoride contaminated waters, a variety of methods have been developed, including adsorption, precipitation, ion-exchange, electrodialysis and reverse osmosis. Among these methods, adsorption is still one of the most extensively used methods, because of its simplicity and the availability of a wide range of adsorbents. Various materials such as functionalized pumice stone (Asgari et al., 2012), Zr(IV)-ethylenediamine (Mohapatra et al., 2012), Mg-doped nano ferrihydrite (Swain et al., 2012), red mud (Cengeloglu et al., 2002), nano-alumina (Kumar et al., 2011), Fe-Al-Ce trimetal oxide (Wu et al., 2007), neodymium-modified chitosan (Yao et al., 2009), and others, have been successfully tested for defluoridation of drinking water.

Response surface methodology (RSM) is a collection of mathematical and statistical techniques useful for analyzing the effects of several independent variables (Myers and Montgomery, 2002). RSM can help in investigating the interactive effect of process variables and in building a mathematical model that accurately describes the overall process. The most common and efficient design used in response surface modeling is the Box-Behnken design. Compared to the central composite and Doehlert designs, Box-Behnken presents some advantages such as requiring few experimental points for its application (three levels per factor) and high efficiency (Ferreira et al., 2007). Several studies used successfully the Box-Behnken design such as the adsorption of methylene blue by kapok fiber treated by sodium chlorite (Liu et al., 2012), the Cr(VI) adsorption onto activated carbons (Ozdemir et al., 2011), the degradation of Acid Red 274 using H<sub>2</sub>O<sub>2</sub> in subcritical water (Kayan and Gozmen, 2012), the removal of fluoride from aqueous solution by adsorption on Apatitic tricalcium phosphate (Mourabet et al., 2012), and more.

In the present work, the combined effect of adsorbent dose, pH, initial concentration and temperature on fluoride removal from aqueous medium by Brushite was investigated using Box-Behnken design in response surface methodology (RSM) by Design Expert Version 8.0.7.1 (Stat Ease, USA). The experimental data were analyzed by fitting to a second order polynomial model, which was statistically validated by performing Analysis of Variance (ANOVA) and lack-of-fit test to evaluate the significance of the model. Moreover, fluoride adsorption was also evaluated with the aspect of kinetics and isotherms.

## 2. Materials and method

### 2.1. Adsorbent

Brushite was prepared by an aqueous double decomposition of the salt of calcium and of phosphate salt (Jones and Smith, 1962). The pH of the zero point charge (pH<sub>Z</sub>) of adsorbent was found to be 6, 2 (Mourabet et al., 2011). The XRD pattern of synthesized Brushite and the sample treated with fluoride are presented in Fig. 1. There is no major change in the XRD pattern of adsorbent after fluoride treatment, only the intensity of the peaks. The surface condition and the existence of fluoride onto Brushite were confirmed by the SEM with EDX analysis. Fig. 2a and b shows the SEM images before and after fluoride adsorption with Brushite. The changes in the surface morphology of Brushite before and after fluoride treatment indicate fluoride adsorption on Brushite. The EDX

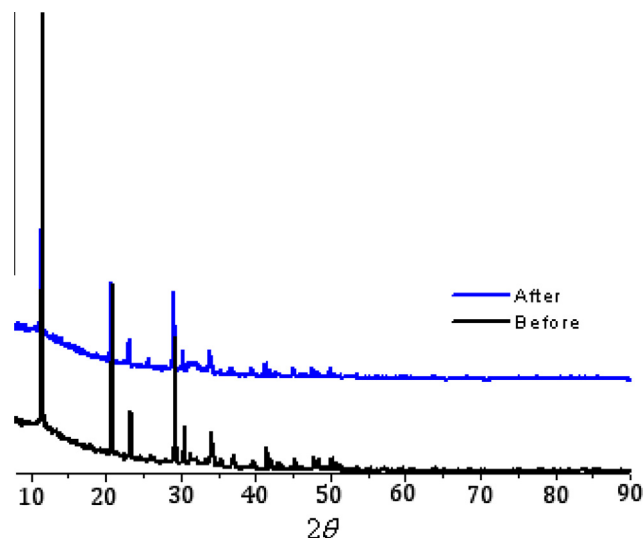


**Figure 1** XRD of Brushite before and after adsorption of fluoride.

spectrum of Brushite confirms the elements present in it and is shown in Fig. 2c. The presence of a fluoride peak in the EDX spectra of fluoride-adsorbed Brushite confirms the fluoride adsorption onto Brushite which is shown in Fig. 2d. The EDX analysis showed that the calcium content decreases after fluoride treatment. The Ca deficiency in Brushite crystals has been attributed to the formation of CaF<sub>2</sub> (Sekar and Suguna, 2011).

### 2.2. Adsorption experiments

The batch equilibration method was followed for the optimization process according to the Box-Behnken design matrix shown in Tables 1 and 2. For this, 100 mL of fluoride aqueous solution with different pH, initial concentration, temperature and adsorbent dose was placed in a 125 mL glass bottle. The mixture was agitated at 200 rpm and at fixed contact time (120 min) that was obtained from kinetic study. The solution was then filtered and the residual fluoride ion concentration analyzed electrochemically with a fluoride ion-selective electrode (Orion, USA) by the use of total ionic strength adjustment buffer (TISAB) solution. Amount of fluoride adsorbed,  $q_e$ (mg/g) was determined using the equation

$$q_e = \frac{(C_0 - C_e)V}{m} \quad (1)$$

where  $C_0$  is initial fluoride concentration (mg/L);  $C_e$ , the equilibrium fluoride concentration (mg/L);  $V$ , volume of fluoride solution (L); and  $m$ , the mass of Brushite (g). Fluoride removal (%) by Brushite was calculated as the ratio of difference in initial and final fluoride concentration ( $C_0 - C_e$ ) to initial fluoride concentration ( $C_0$ )

$$y(\%) = \frac{C_0 - C_e}{C_0} \times 100 \quad (2)$$

where  $C_0$  and  $C_e$  are the initial and equilibrium concentrations of fluoride in the solutions in mg/L respectively.

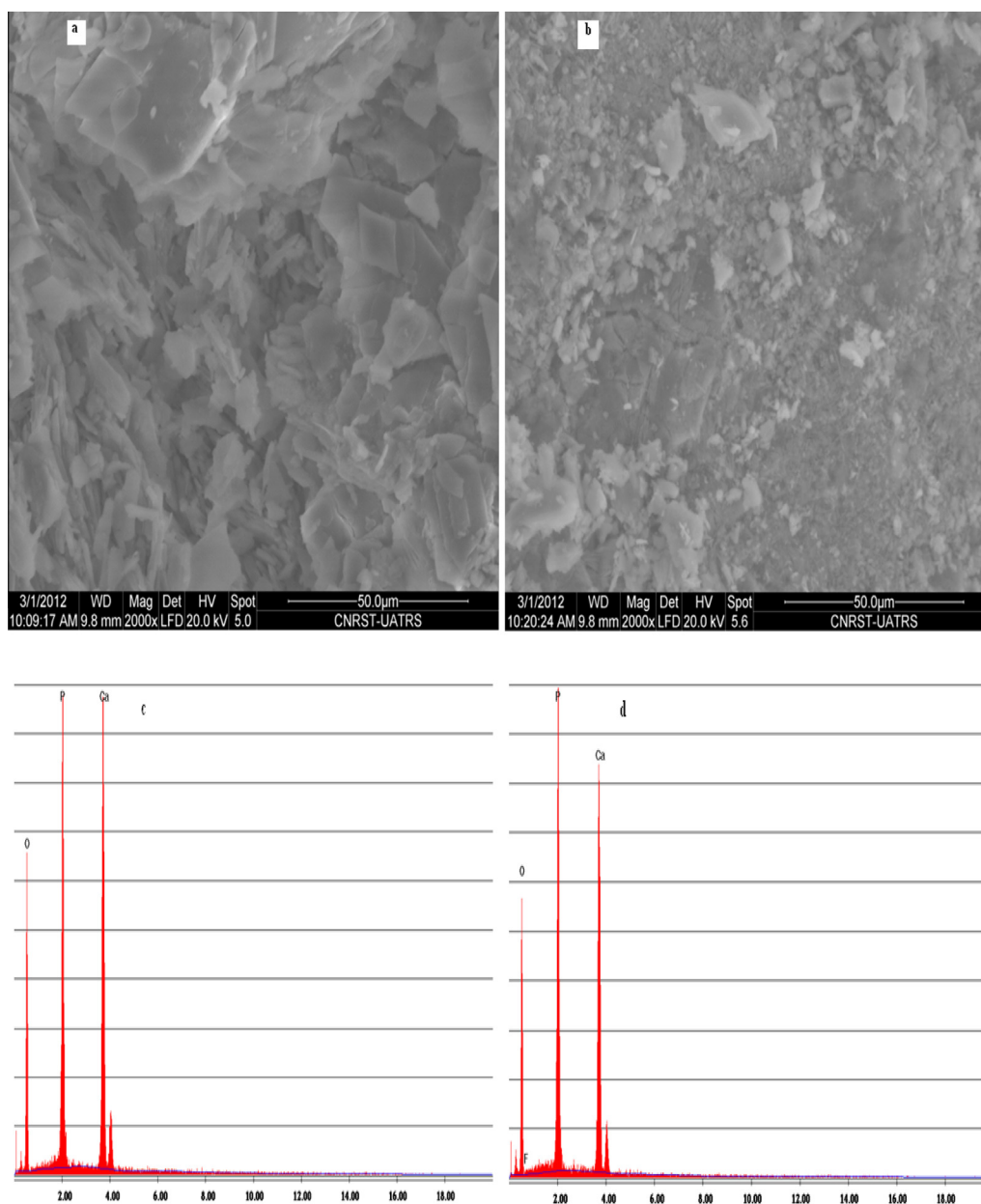


**Figure 2** SEM images of (a) Brushite and (b) fluoride-adsorbed Brushite and EDX spectra of (c) Brushite and (d) fluoride-adsorbed Brushite.

### 2.3. Box–Behnken experimental design

Box–Behnken statistical experiment design and the response surface methodology were employed to investigate the effects of the four independent variables on the response function. The independent variables were initial concentrations of fluoride ( $X_1$ ), pH ( $X_2$ ), adsorbent dose ( $X_3$ ) and temperature ( $X_4$ ). The low, center and high levels of each variable are designated as  $-1$ ,  $0$ , and  $+1$ , respectively as illustrated in Table 1. The experimental levels for each variable were selected based on results from preliminary experiments. The response function was percent fluoride adsorption.

Coding of the variables was done according to the following equation:

$$x_i = \frac{(X_i - X_0)}{\Delta X_i} \quad (3)$$

where  $x_i$  is the dimensionless value of an independent variable,  $X_i$  is the real value of an independent variable,  $X_0$  is the real value of an independent variable at the center point, and  $\Delta X_i$  is the step change of the real value of the variable  $i$  corresponding to a variation of a unit for the dimensionless value of the variable  $i$ . The number of experiments ( $N$ ) needed for the development of Box–Behnken matrix is defined as  $N = 2k(k-1) + r$ , where ( $k$ ) is the factor number and ( $r$ ) is the replicate number of the central point.

A total of 29 experiments have been employed in this work to evaluate the effects of the four main independent

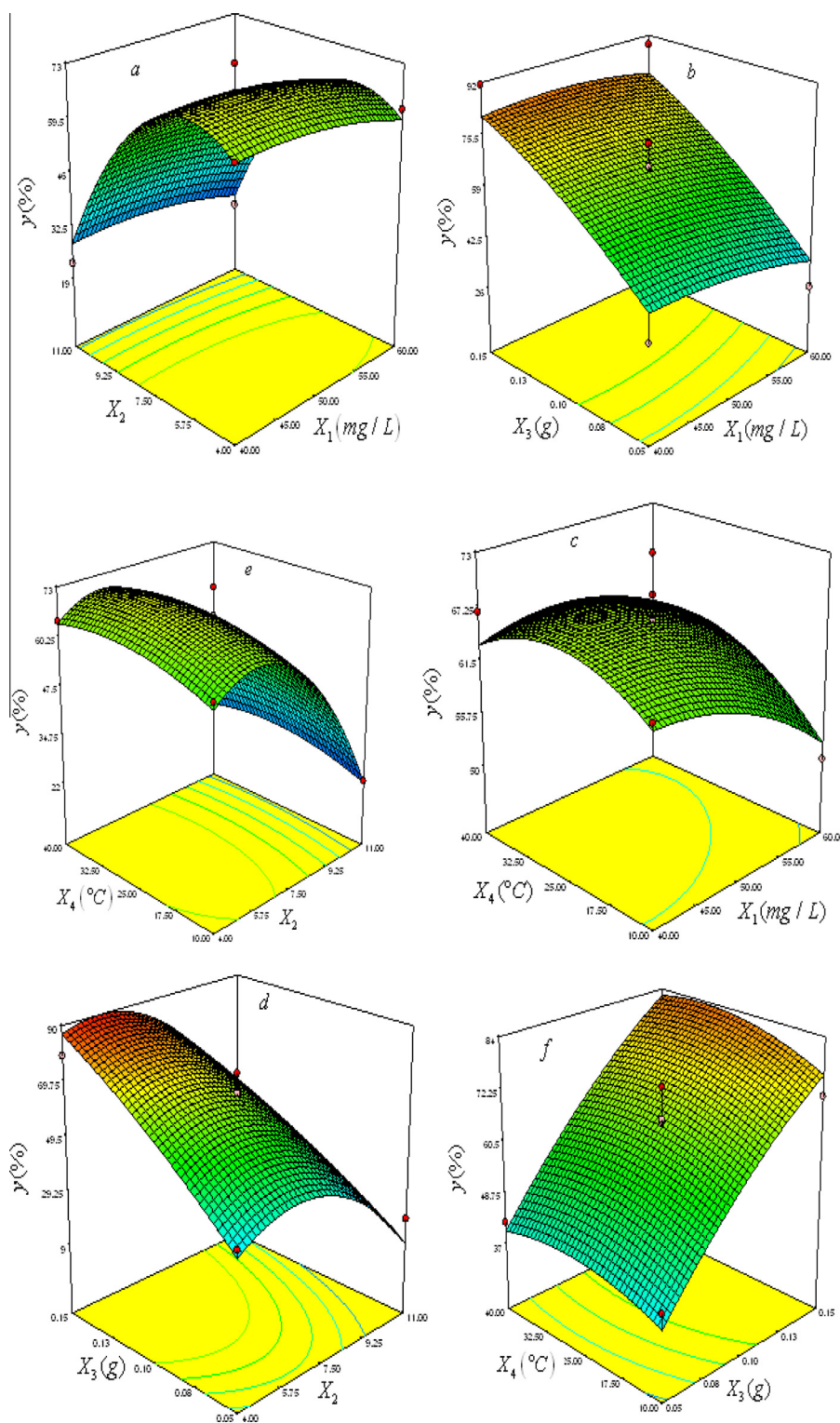


**Figure 3** Response surface plots for fluoride removal efficiency (%) onto Brushite: (a) effect pH/initial concentration (adsorbent dose 0.1 g, temperature 25 °C); (b) effect temperature/initial concentration (pH 7.50, adsorbent dose 0.1 g); (c) effect pH/adsorbent dose (temperature 25, Initial concentration 50 mg/L); (d) effect temperature/adsorbent dose (pH 7.50, initial concentration 50 mg/L); (e) effect temperature/pH (initial concentration 50 mg/L, adsorbent dose 0.1 g); and (f) effect initial concentration/adsorbent dose (pH 7.50, temperature 25 °C).

parameters on fluoride adsorption efficiency. The actual experimental design matrix is given in Table 2.

The performance of the process was evaluated by analyzing the response ( $y$ ), which depends on the input factors  $X_1$ ,  $X_2$ ,

**Table 1** Independent variables and their levels used for Box–Behnken design.

Variables, unit	Factors	Levels		
	$X$	-1	0	1
Initial concentrations of fluoride(mg/L)	$X_1$	40	50	60
pH	$X_2$	4	7.5	11
Adsorbent dose(g)	$X_3$	0.05	0.1	0.15
Temperature(°C)	$X_4$	10	25	40

**Table 2** Box–Behnken experimental design matrix and experimental responses.

Experimental run	$X_1$	$X_2$	$X_3$	$X_4$	$y$ (%)
1	+1.00	0.00	0.00	-1.00	50.78
2	0.00	0.00	+1.00	-1.00	70.96
3	0.00	-1.00	0.00	+1.00	64.40
4	0.00	+1.00	+1.00	0.00	38.08
5	-1.00	0.00	-1.00	0.00	35.45
6	+1.00	0.00	-1.00	0.00	26.43
7	-1.00	+1.00	0.00	0.00	23.05
8	0.00	-1.00	+1.00	0.00	79.22
9	-1.00	-1.00	0.00	0.00	65.55
10	0.00	0.00	0.00	0.00	64.40
11	0.00	+1.00	-1.00	0.00	18.92
12	+1.00	0.00	+1.00	0.00	88.83
13	0.00	+1.00	0.00	+1.00	25.64
14	0.00	0.00	0.00	0.00	72.92
15	-1.00	0.00	0.00	-1.00	63.05
16	-1.00	0.00	+1.00	0.00	91.25
17	0.00	0.00	-1.00	-1.00	40.64
18	0.00	0.00	0.00	0.00	65.30
19	0.00	0.00	+1.00	+1.00	76.32
20	0.00	+1.00	0.00	-1.00	22.50
21	+1.00	-1.00	0.00	0.00	61.75
22	-1.00	0.00	0.00	+1.00	66.77
23	0.00	-1.00	-1.00	0.00	38.64
24	+1.00	0.00	0.00	+1.00	62.21
25	+1.00	+1.00	0.00	0.00	19.73
26	0.00	-1.00	0.00	-1.00	60.36
27	0.00	0.00	0.00	0.00	61.54
28	0.00	0.00	0.00	0.00	65.74
29	0.00	0.00	-1.00	+1.00	42.00

...,  $X_k$ , and the relationship between the response and the input process parameters is described by

$$y = f(X_1, X_2, \dots, X_k) + \varepsilon \quad (4)$$

where  $f$  is the real response function the format of which is unknown and  $\varepsilon$  is the residual factor associated with the experiments.

The surface represented by  $f(X_i, X_j)$  is called a response surface. The response can be represented graphically, either in the three-dimensional space or as contour plots that help visualize the shape of the response surface.

For RSM, the most commonly used second-order polynomial equation developed to fit the experimental data and determine the relevant model terms can be written as:

$$y = \beta_0 + \sum \beta_i X_i + \sum \beta_{ii} X_i^2 + \sum \beta_{ij} X_i X_j \quad (5)$$

where  $\beta_0$  is the constant coefficient,  $\beta_i$  is the slope or linear effect of the input factor  $X_i$ ,  $\beta_{ij}$  is the linear by linear interaction effect between the input factor  $X_i$  and,  $\beta_{ii}$  is the quadratic effect of input factor  $X_i$ .

#### 2.4. Desirability function

The desirability function approach is a technique for the simultaneous determination of optimum settings of input variables that can determine optimum performance levels for one or more responses. The desirability procedure involves two steps: (1) finding the levels of the independent variables that simultaneously produce the most desirable predicted responses on the dependent variables and (2) maximize the overall desirability with respect to the controllable factors. The desirability function approach was originally introduced by Harrington (1965). Then another version was developed by Derringer and Suich (1980). The general approach is to first convert each response ( $y_i$ ) into an individual desirability function ( $d_i$ ) varying over the range

$$0 \leq d_i \leq 1 \quad (6)$$

where if response  $y_i$  is at its goal or target, then  $d_i = 1$ , and if the response is outside an acceptable region,  $d_i = 0$ . Then the design variables are chosen to maximize the overall desirability

$$D = (d_1 \times d_2 \times \dots \times d_n)^{\frac{1}{n}} \quad (7)$$

where  $n$  is the number of responses in the measure.

Depending on whether a particular response  $y_i$  is to be maximized, minimized or assigned a target value, the different desirability functions  $d_i(y_i)$  used are those proposed by Derringer and Suich (1980).

If a response is of the “target is the best” kind, then its individual desirability function is:

$$\begin{cases} d_i = (y_i - L_i / T_i - L_i)^p & \text{if } L_i \leq y_i \leq T_i \\ d_i = (y_i - U_i / T_i - U_i)^q & \text{if } L_i \leq y_i \leq T_i \\ d_i = 1 & \text{if } y_i = T_i \\ d_i = 0 & \text{if } y_i = L_i \text{ or } y_i = L_i \end{cases} \quad (8)$$

with the exponents  $p$  and  $q$  determining how important it is to hit the target value.

If a response is to be maximized instead, the individual desirability is defined as shown in Eq. (9).

$$\begin{cases} d_i = 0 & \text{if } y_i \leq L_i \\ d_i = (y_i - L_i / T_i - L_i)^p & \text{if } L_i \leq y_i \leq T_i \\ d_i = 1 & \text{if } y_i \geq T_i \end{cases} \quad (9)$$

Finally, if a response is to be minimized, the individual desirability ( $d_i$ ) is calculated according to Eq. (10).

$$\begin{cases} d_i = 1 & \text{if } y_i \leq T_i \\ d_i = (y_i - U_i/T_i - U_i)^q & \text{if } T_i \leq y_i \leq U_i \\ d_i = 0 & \text{if } y_i \geq U_i \end{cases} \quad (10)$$

where  $L_i$ ,  $U_i$  and  $T_i$  are the lower, upper and target values, respectively, that are desired for response  $y_i$ , with  $L_i \leq y_i \leq U_i$ .

### 2.5. Adsorption isotherms

There are many equations for analyzing experimental adsorption equilibrium data. In this work, the following three models were tested:

The Langmuir isotherm theory assumes monolayer coverage of adsorbate over a homogenous adsorbent surface. The Langmuir (1916) equation is formulated as

$$q_e = \frac{Q_L b C_e}{1 + b C_e} \quad (11)$$

where  $Q_L$  is the maximum adsorption capacity of the adsorbent (mg/g), corresponding to monolayer surface coverage, and  $b$  is the adsorption affinity constant or the Langmuir constant (L/mg) and is a measure of the energy of adsorption.

The Freundlich (1907) isotherm is an empirical equation describing the adsorption onto a heterogeneous surface. The Freundlich isotherm is commonly presented as Eq. (12).

$$q_e = K_F C_e^{1/n} \quad (12)$$

where  $K_F$  is the Freundlich constant related with adsorption capacity ( $\text{mg g}^{-1}(\text{mg L}^{-1})^{-1/n}$ ) and  $n$  is the Freundlich exponent (dimensionless).

The Sips model is a combination of the Langmuir and Freundlich isotherm type models. The Sips model takes the following form (Sips, 1948):

$$q_e = \frac{Q_S K_S C_e^{1/s}}{1 + K_S C_e^{1/s}} \quad (13)$$

where  $K_S$  constant is related to affinity constant ( $\text{mg L}^{-1})^{-1/n}$ ,  $Q_S$  is the Sips maximum adsorption capacity (mg/g) and  $1/s$  is the heterogeneity factor. If the value for  $1/s$  is less than one, it indicates that it is heterogeneous adsorbents, while values closer to or even one indicates that the adsorbent has relatively more homogeneous binding sites.

### 2.6. Adsorption kinetics

In order to examine the controlling mechanism of adsorption processes, pseudo-first-order, pseudo-second-order, and intra-particle diffusion kinetic equations were used to test the experimental data. The pseudo-first-order equation of Lagergren (1898) is generally expressed as Eq. (14):

$$q_t = q_e(1 - \exp(-k_1 t)) \quad (14)$$

where  $k_1$  ( $\text{min}^{-1}$ ) is the rate constant of pseudo-first-order adsorption.

The pseudo-second-order equation based on adsorption equilibrium capacity can be expressed as Eq. (15) (Ho and McKay, 1998):

$$q_t = \frac{k_2 q_e^2 t}{1 + k_2 q_e t} \quad (15)$$

where  $k_2$  ( $\text{g}/(\text{mg min})$ ) is the rate constant of pseudo-second-order adsorption.

The intra-particle diffusion model (Weber and Morris, 1963) was applied to the kinetic data with the pore diffusion factor described by Eq. (16):

$$q_t = k_i \sqrt{t} + c \quad (16)$$

where  $k_i$  is the intra-particle diffusion rate constant ( $\text{mg g}^{-1} \text{min}^{1/2}$ ) and  $c$  is the intercept ( $\text{mg/g}$ ).

### 2.7. Regression analysis, goodness-of-fit measure and model comparison

All the model parameters were evaluated by non-linear regression using MATLAB software. Apart from the determination coefficient ( $R^2$ ), the sum of squares due to error (SSE), the residual root mean square error (RMSE) and the chi-square test were also used to measure the goodness-of-fit. We used one statistical approach for comparing models: the second-order corrected Akaike Information Criterion ( $AIC_C$ ).

These error functions employed are as follows:

- (i) The sum of the square of the errors (SSE):

$$SSE = \sum_{i=1}^n (q_{i(\text{exp})} - q_{i(\text{mod})})^2 \quad (17)$$

where  $q_{i(\text{exp})}$  is the adsorption capacity obtained from experiment,  $q_{i(\text{mod})}$  is the adsorption capacity obtained from kinetic model.

- (i) The coefficient of determination ( $R^2$ ):

$$R^2 : R^2 = 1 - \frac{SSE}{SST} \quad (18)$$

where  $SSE$  is called the sum of the square of the errors and  $SST$  is called the total sum of squares

- (i) The residual root mean square error (RMSE):

$$RMSE = \sqrt{\frac{1}{n-p} \sum_{i=1}^n (q_{i(\text{exp})} - q_{i(\text{mod})})^2} \quad (19)$$

- (i) The chi-square test:

$$\chi^2 = \sum_{i=1}^n \frac{(q_{i(\text{exp})} - q_{i(\text{mod})})^2}{q_{i(\text{mod})}} \quad (20)$$

- (i) The corrected Akaike information criterion ( $AIC_C$ )

$$AIC_C = n \ln \frac{SSE}{n} + 2p + \frac{2p(p+1)}{n-p-1} \quad (21)$$

where  $p$  is the number of parameters in the model, and  $n$  the number of data points.  $AIC_C$  values can be compared using the Evidence ratio ( $E$ ) which is defined by:

$$E = \frac{1}{\exp(-0.5\Delta)} \quad (22)$$

where  $\Delta$  is the absolute value of the difference in  $AIC_C$  between the two models.

### 3. Results and discussions

#### 3.1. Box–Behnken statistical analysis

The Box–Behnken responses were analyzed and the results of ANOVA for adsorption study of fluoride are presented in Table 3.

The analysis of variance is essential to test significance and adequacy of the model. It subdivides the total variation of the results in two sources of variation, the model and the experimental error, shows whether the variation from the model is significant when compared to the variation due to residual error (Seguro et al., 1999). Fisher's  $F$ -test value, which is the ratio between the mean square of the model and the residual error, performs this comparison (Kasiri et al., 2013; Khataee et al., 2010). As shown in Table 3, the  $F$ -value obtained, 16.56, is greater than the  $F$  value (2.47 at 95% significance) obtained from the standard distribution table, confirming the adequacy of the model fits. The significance of each term was determined by  $p$ -value (Prob >  $F$ ), which is listed in Table 2. As seen in this table the terms  $X_2$ ,  $X_3$ , and  $X_2^2$ , were significant, with very small  $p$ -values ( $p < 0.05$ ). The other term coefficients were not significant ( $p > 0.05$ ).

The “Lack of Fit Test” compares the residual error to the pure error from replicated design points. The lack of fit  $F$ -value of 3.63 is not significant as the  $p$ -value is  $> 0.05$ . The non-significance lack-of-fit showed that the model was valid for the present work.

The resulting RSM model equation is following:

$$y(\%) = -87.09 + 1.5 \times X_1 + 21.72 \times X_2 + 715.7 \times X_3 + 0.22 \times X_4 + 3.42 \times 10^{-3} \times X_1 X_2 + 3.3 \times X_1 X_3 + 0.012 \times X_1 X_4 - 30.6 \times X_2 X_3 - 4.28 \times 10^{-3} \times X_2 X_4 + 1.33 \times X_3 X_4 - 0.024 \times X_1^2 - 1.60 \times X_2^2 - 1401.16 \times X_3^2 - 0.016 \times X_4^2 \quad (23)$$

From Eq. (23), it can be seen that the initial concentration, pH, adsorbent dose, and temperature have positive effect on the percent fluoride adsorption. A positive value represents an effect that favors the optimization, while a negative value indicates an inverse relationship between the factor and the response.

The Pareto analysis (Khuri and Cornell, 1996) was carried out to check the percentage effect of each factor. In fact, this analysis calculates the percentage effect ( $P_i$ ) of each factor on the response, according to the following relation:

$$P_i = \left( \frac{\beta_i^2}{\sum_{i=1}^{14} \beta_i^2} \right) \times 100 (i \neq 0) \quad (24)$$

where  $\beta_i$  is the regression coefficient of individual process variable.

Fig. 4 shows the Pareto graphic analysis. As can be seen in this figure, among the variables, the adsorbent dose ( $\beta_3$ , 20.68% and  $\beta_3^2$ , 79.26%) produces the main effect on the percent fluoride adsorption.

The coefficient of determination ( $R^2$ ) of the model was 0.9430, which indicated a good fit between predicted values and the experimental data points (Fig. 5). In addition, this implies that 94.3% of the variations for percent fluoride adsorption are explained by the independent variables, and this also means that the model does not explain only about 5.7% of variation. Predicted  $R^2$  is a measure of how good the model predicts a response value. The adjusted  $R^2$  and predicted  $R^2$

**Table 3** Analysis of variance (ANOVA) for Response Surface Quadratic Model.

Source	Sum of Squares	df	Mean square	F Value	p-Value (Prob > F)
Model	11836.09	14	845.44	16.56	< 0.0001
$X_1$	104.37	1	104.37	2.04	0.1748
$X_2$	4107.00	1	4107.00	80.43	< 0.0001
$X_3$	4903.75	1	4903.75	96.03	< 0.0001
$X_4$	70.33	1	70.33	1.38	0.2602
$X_1 X_2$	0.058	1	0.058	1.128E-003	0.9737
$X_1 X_3$	10.89	1	10.89	0.21	0.6513
$X_1 X_4$	0.06	1	0.06	0.29	0.5980
$X_2 X_3$	114.70	1	114.70	2.25	0.1561
$X_2 X_4$	0.20	1	0.20	3.966E-003	0.9507
$X_3 X_4$	4.00	1	4.00	0.078	0.7837
$X_1^2$	40.19	1	40.19	0.79	0.3900
$X_2^2$	2495.77	1	2495.77	48.87	< 0.0001
$X_3^2$	79.59	1	79.59	1.56	0.2323
$X_4^2$	86.02	1	86.02	1.68	0.2153
Residual	714.90	14	51.06		
Lack of fit	644.01	10	64.40	3.63	0.1126
Pure error	70.89	4	17.72		
Cor total	12551.00	28			

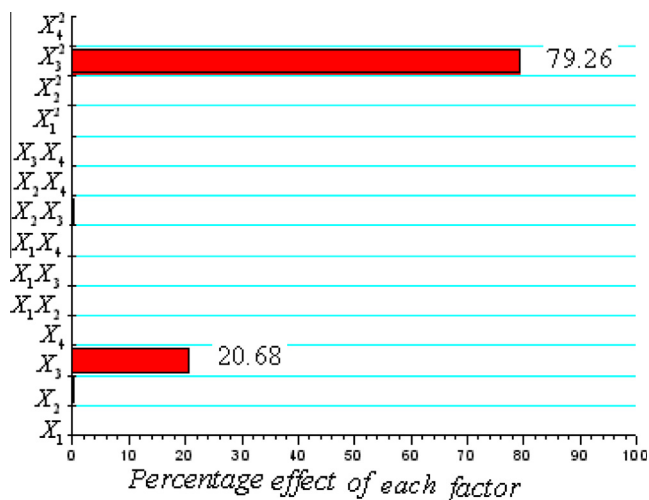


Figure 4 Pareto graphic analysis.

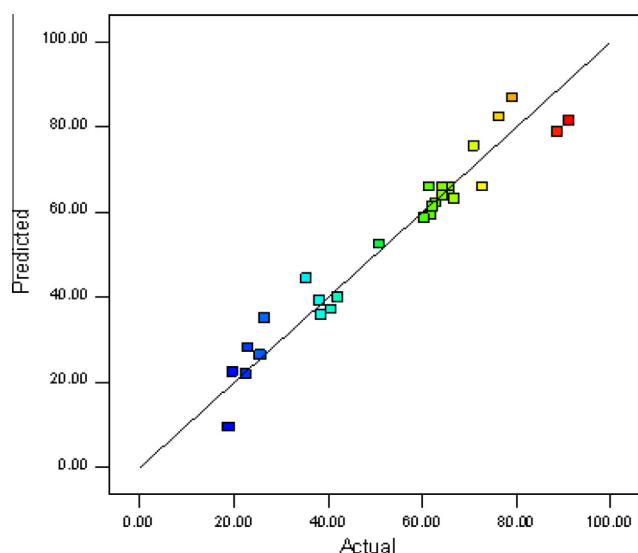


Figure 5 Plot of the experimental and predicted responses.

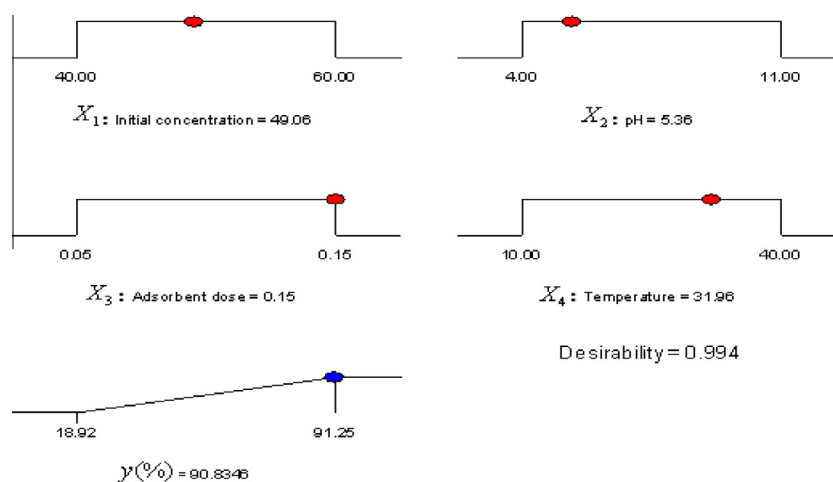


Figure 6 Desirability ramp for optimization.

should be within  $\sim 0.20$  of each other to be in reasonable agreement. If they are not, there may be a problem with either the data or the model. In our case, the predicted  $R^2$  of 0.6965 is in reasonable agreement with the adjusted  $R^2$  of 0.8861. Adequate precision measures the signal to noise ratio and compares the range of the predicted values at the design points to the average prediction error. The ratio greater than 4 is desirable and indicates adequate model discrimination. In this work the ratio is found to be 15.066, which indicates the reliability of the experiment data. The coefficient of variation (CV = 13.26) and standard deviation (SD = 7.15) indicate the degree of precision. The low values of CV and SD show the adequacy with which the experiment is conducted.

The models have high  $R^2$  value, significant  $F$ -value, an insignificant lack-of-fit  $P$ -value and low standard deviation and coefficient of variance. These results indicate the high precision in predicting the fluoride removal efficiency by Brushite. Therefore, the models were used for further analysis.

### 3.2. Effect of interactive variables

The response surface plots of the second-order polynomial equation with two variables were kept constant and the other two varying within the determined experimental ranges are given in Fig. 3.

Fig. 3a, c and e present response surface plots of the effect of pH and initial fluoride concentration, pH and adsorbent dose, and pH and temperature respectively on the adsorption of fluoride onto Brushite respectively. It shows that Fluoride removal efficiency increased with decreasing initial pH. This observation can be explained on the basis of zero point of charge for adsorbent ( $pH_Z = 6.2$ ). Brushite surface has positive charge when solution pH is less than  $pH_Z$ , thus the fluoride removal efficiency increases. In the solution with  $pH > pH_Z$ , Brushite surface becomes negatively charged and decreases the fluoride removal. Fig. 3f depicts the contour response surface plots showing the effect of adsorbent dosage and initial fluoride concentration on fluoride removal efficiency for Brushite. The fluoride removal efficiency of Brushite was increased with an increase in initial fluoride concentration at 40–50 mg/L but further increase in adsorbate concentration shows a slight decrease. Fluoride removal efficiency increases



along with an increase in adsorbent dosage from 0.05 to 0.15 g for Brushite. Also, the increase in fluoride removal efficiency with increasing amount of adsorbent is shown in Fig. 3(c and d). The reason for this observation may be due to availability of more vacant binding sites to adsorbate on the surface of adsorbent. The response surface plots in Fig. 3b, d and e show that fluoride removal efficiency increased with increasing temperature from 10 to 40 °C, which indicates that the adsorption process was endothermic in nature.

### 3.3. Optimization using the desirability function

By using numerical optimization, a desirable value for each input factor and response can be selected. Therein, the possible input optimizations that can be selected include: the range, maximum, minimum, target, none (for responses) and set so as to establish an optimized output value for a given set of conditions. In this study, the input variables were given specific ranged values, whereas the response was designed to achieve a maximum. Using these conditions, the maximum achieved fluoride removal efficiency was 90.83% (Fig. 6) at an initial pH of 5.36, fluoride concentration of 49.06 mg/L, adsorbent dose of 0.15 g, and temperature of 31.96 °C. The confirmatory experiment showed a fluoride removal efficiency of 88.78% under optimal conditions compared with the fluoride removal percent of 90.83% obtained by the model. This indicates the suitability and accuracy of the model.

### 3.4. Adsorption kinetics and isotherms

Fig. 7 illustrates the isotherm models that are fitted to the experimental data obtained at 20 °C. Similar trends were also obtained at 30 and 40 °C (results not shown). The determined error function values and isotherm parameters obtained for all temperatures are shown in Table 4. According to Table 4, the Langmuir and Sips isotherm show a better fit to the adsorption data than the Freundlich isotherm in the adsorption of fluoride basing on the highest  $R^2$  value and the lowest  $SSE$ ,  $RMSE$ , and  $\chi^2$  values. At  $T = 293$  K,  $AIC_C$  values were calculated for Langmuir (-3.638) and Sips (2.378) isotherms. Having a

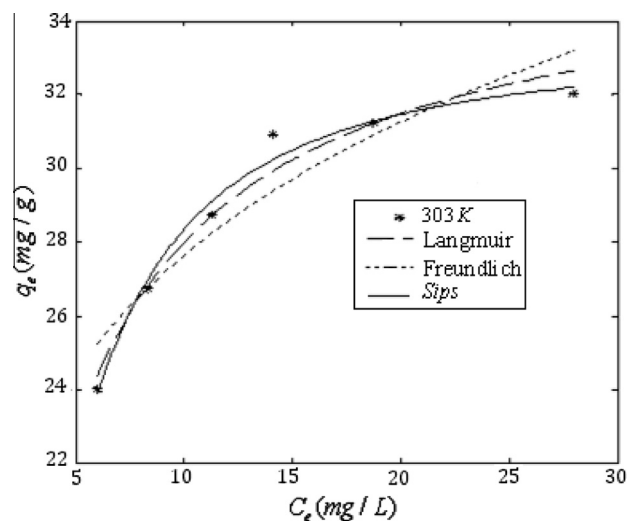


**Figure 7** Adsorption isotherms of fluoride onto Brushite at  $T = 303$  K.

**Table 4** Isotherm parameters for the adsorption of fluoride by Brushite.

Langmuir	293 K	303 K	313 K
$Q_L$	29.212	35.952	36.260
$b$	0.217	0.352	2.336
$R^2$	0.961	0.968	0.975
$SSE$	0.862	1.500	0.949
$RMSE$	0.064	0.612	0.487
$\chi^2$	0.036	0.049	0.027
$AIC_C$	-3.638	0.405	-0.025
<i>Freundlich</i>			
$K_F$	13.130	18.378	28.545
$\frac{1}{n}$	0.193	0.177	0.078
$R^2$	0.896	0.884	0.971
$SSE$	2.355	5.538	3.172
$RMSE$	0.767	1.176	0.890
$\chi^2$	0.1007	0.192	0.102
$AIC_C$	2.611	1.711	0.154
<i>Sips</i>			
$Q_S$	26.537	33.288	36.072
$K_S$	0.053	0.147	2.338
$\frac{1}{s}$	1.725	1.590	0.867
$R^2$	0.980	0.985	0.967
$SSE$	0.444	0.703	0.902
$RMSE$	0.384	0.484	0.548
$\chi^2$	0.0196	0.023	0.027
$AIC_C$	2.378	-0.351	-0.102

smaller  $AIC_C$  value suggests that Langmuir isotherm is more likely to be a better fit. The evidence ratio of 20.24 means that it is 20.24 times more likely to be the correct model than the Sips isotherm. Therefore, the experimental results suggest that a monolayer of fluoride ions is adsorbed on homogeneous adsorption sites on the surface of Brushite. The Langmuir maximum adsorption monolayer capacities were found to be 29.212, 35.952 and 36.260 at 298 K, 303 K, and 313 K respectively. Clearly, from these values, Brushite examined in this study demonstrates the highest adsorption capacity in comparison to most other adsorbents in terms of defluoridation capac-

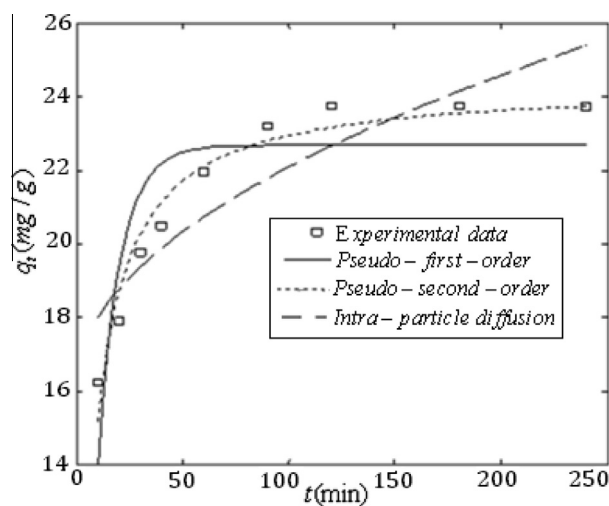


**Figure 8** Adsorption kinetics of fluoride onto Brushite at 30 mg/L.

**Table 5** Kinetic parameters for the adsorption of fluoride by Brushite.

Pseudo-first-order	30 mg/L	40 mg/L
$q_e$	22.547	26.640
$k_1$	0.094	0.192
$R^2$	0.667	0.639
$SSE$	21.894	6.262
$RMSE$	1.766	0.945
$\chi^2$	1.147	0.245
$AIC_C$	13.982	1.834
<i>Pseudo-second-order</i>		
$q_e$	24.349	27.58
$k_2$	0.0068	0.192
$R^2$	0.951	0.639
$SSE$	2.997	0.639
$RMSE$	0.654	6.662
$\chi^2$	0.162	0.245
$AIC_C$	-3.984	1.834
<i>Intra-particle diffusion</i>		
$q_e$	15.706	23.56
$k_i$	0.626	10.303
$R^2$	0.833	0.737
$SSE$	10.939	4.519
$RMSE$	1.250	0.809
$\chi^2$	0.519	0.180
$AIC_C$	7.756	1.524

ity (Kumar et al., 2011, 2009; Viswanathan and Meenakshi, 2008; Biswas et al., 2007).

The adsorption kinetic was studied at temperature: 25 °C; initial fluoride concentration: 30 and 40 mg/L; adsorbent dose: 0.1 g and pH: (6.8–6.9). Fig. 8 illustrates the kinetic models that are fitted to the experimental data. Similarly, all values of different kinetic parameters, as shown in Table 5, were obtained from various graphical presentations of kinetic equations. Analyzing the data, it can be mentioned that the highest  $R^2$  value and the lowest  $SSE$ ,  $RMSE$ ,  $\chi^2$  and  $AIC_C$  values were found for the pseudo-second-order kinetic model. In addition, the values of  $q_{e,exp}$  (23.75–27.33 mg/g) and  $q_{e,cal}$  (24.34–27.58 mg/g) are also found to be very close to each other. Therefore, the adsorption is expected to follow pseudo-second-order kinetic.

#### 4. Conclusions

In this study, the statistical methodology, Box–Behnken Response Surface design is demonstrated to be effective and reliable in finding the optimal conditions for the adsorption of fluoride onto Brushite. The results showed that, the adsorption conditions have significant effects on the removal of fluoride. The response surface plots were used for estimating the interactive effect of four independent variables (initial fluoride concentration, pH, temperature and adsorbent dose) on the response (percent fluoride adsorption). The second order mathematical model was developed by regression analysis of the experimental data obtained from 29 batch runs. Applying the method of the desirability function, optimization of adsorbent dose (0.15 g), initial concentration (49.06 mg L<sup>-1</sup>),  $T$  (31.96 °C) and pH (5.36) gave a maximum of 90.83% fluoride removal with desirability of 0.994. Different kinetic models were also examined, and the pseudo-second order was found

to be the applicable kinetic model in the present study. The Langmuir, Freundlich, and Sips adsorption isotherm models were used for the description of the adsorption equilibrium of fluoride. The data were in good agreement with Langmuir isotherm. This study demonstrated that the Brushite has relatively high adsorption capacity compared to some other adsorbents reported in the literature.

#### References

- Asgari, G., Roshani, B., Ghanizadeh, G., 2012. The investigation of kinetic and isotherm of fluoride adsorption onto functionalize pumice. *J. Hazard. Mater.* 217, 123–132.
- Biswas, K., Bandhoyapadhyay, D., Ghosh, U.C., 2007. Adsorption kinetics of fluoride on iron(III)–zirconium(IV) hybrid oxide. *Adsorption* 13, 83–94.
- Cengeloglu, Y., Kir, E., Ersoz, M., 2002. Removal of fluoride from aqueous solution by using red mud. *Sep. Purif. Technol.* 28, 81–86.
- Derringer, G., Suich, R., 1980. Simultaneous optimization of several response variables. *J. Quality Technol.* 12, 214–219.
- Ferreira, S.L., Bruns, R.E., Ferreira, H.S., Matos, G.D., David, J.M., Brandao, G.C., da Silva, E.G., Portugal, L.A., dos Reis, P.S., Souza, A.S., dos Santos, W.N., 2007. Box–Behnken design: an alternative for the optimization of analytical methods. *Anal. Chim. Acta.* 597, 179–186.
- Freundlich, H., 1907. Über die adsorption in Lösungen. *Zeitschrift für Physikalische Chemie* 57, 385–470.
- Harrington Jr., E.C., 1965. The desirability function. *Ind. Qual. Control* 21, 494–498.
- Ho, Y.S., McKay, G., 1998. Kinetic model for lead(II) sorption on to peat. *Adsorpt. Sci. Technol.* 16, 243–255.
- Jones, D.W., Smith, J.A.S., 1962. The structure of brushite, CaH<sub>2</sub>PO<sub>4</sub>·2H<sub>2</sub>O. *J. Chem. Soc.*, 1414–1420.
- Kasiri, M.B., Modirshahla, N., Mansouri, H., 2013. Decolorization of organic dye solution by ozonation; optimization with response surface methodology. *Intern. J. Ind. Chem.* 4, 3.
- Kayan, B., Gozmen, B., 2012. Degradation of Acid Red 274 using H<sub>2</sub>O<sub>2</sub> in subcritical water: application of response surface methodology. *J. Hazard. Mater.* 201, 100–106.
- Khataee, A.R., Fathinia, M., Aber, S., Zarei, M., 2010. Optimization of photocatalytic treatment of dye solution on supported TiO<sub>2</sub> nanoparticles by central composite design: intermediates identification. *J. Hazard. Mater.* 181, 886–897.
- Khuri, A.I., Cornell, J.A., 1996. *Response surfaces*, second ed. Dekker, New York.
- Kumar, E., Bhatnagar, A., Ji, M., Jung, W., Lee, S.H., Kim, S.J., Lee, G., Song, H., Choi, J.-Y., Yang, J.-S., Jeon, B.-H., 2009. Defluoridation from aqueous solution by granular ferric hydroxide (FGH). *Water Res.* 43, 490–498.
- Kumar, E., Bhatnagar, A., Kumar, U., Sillanpaa, M., 2011. Defluoridation from aqueous solutions by nano-alumina: characterization and sorption studies. *J. Hazard. Mater.* 186, 1042–1049.
- Lagergren, S., 1898. About the theory of so-called adsorption of soluble substances. *Kungliga Svenska Vetenskapsakademiens Handlingar.* 24, 1–39.
- Langmuir, I., 1916. The constitution and fundamental properties of solids and liquids. *J. Am. Chem. Soc.* 38, 2221–2295.
- Liu, Y., Wang, J., Zheng, Y., Wang, A., 2012. Adsorption of methylene blue by kapok fiber treated by sodium chlorite optimized with response surface methodology. *Chem. Eng. J.* 184, 248–255.
- Mohapatra, M., Hariprasad, D., Mohapatra, L., Anand, S., Mishra, B.K., 2012. Mg-doped nano ferrihydroxide-A new adsorbent for fluoride removal from aqueous solutions. *Appl. Surf. S.* 258, 4228–4236.
- Mourabet, M., El Boujaady, H., El Rhilassi, A., Ramdane, H., Bennani-Ziatni, M., El Hamri, R., Taitai, A., 2011. Defluoridation of water using Brushite: equilibrium, kinetic and thermodynamic studies. *Desalination* 278, 1–9.

- Mourabet, M.El., Boujaady, H., El Rhilassi, A., Bennani-Ziatni, M., El Hamri, R., Taitai, A., 2012. Removal of fluoride from aqueous solution by adsorption on Apatitic tricalcium phosphate using Box–Behnken design and desirability function. *Appl. Surf. Sci.* 258, 4402–4410.
- Myers, R.H., Montgomery, D.C., 2002. *Response Surface 1 Methodology – Process and Product Optimization Using Designed Experiments*, 2nd ed. John Wiley & Sons, New York, NY.
- Ozdemir, E., Duranoglu, D., Beker, U., Avc, A.O., 2011. Process optimization for Cr(VI) adsorption onto activated carbons by experimental design. *Chemi. Eng. J.* 172, 207–218.
- Segurola, J., Allen, N.S., Edge, M., Mahon, A.M., 1999. Design of eutectic photoinitiator blends for UV/visible curable acrylated printing inks and coatings. *Prog. Org. Coat.* 37, 23–37.
- Sekar, C., Suguna, K., 2011. Effect of H<sub>3</sub>PO<sub>4</sub> reactant and NaF additive on the crystallization and properties of brushite. *Adv. Mat. Lett.* 2, 227–232.
- Sips, R., 1948. On the structure of a catalyst surface. *J. Chem. Phys.* 16, 490–495.
- Swain, S.K., Mishra, S., Patnaik, T., Patel, R.K., Jha, U., Dey, R.K., 2012. Fluoride removal performance of a new hybrid sorbent of Zr(IV)–ethylenediamine. *Chem. Eng. J.* 184, 72–81.
- Viswanathan, N., Meenakshi, S., 2008. Selective sorption of fluoride using Fe(III) loaded carboxylated chitosan beads. *J. Fluorine Chem.* 129, 503–550.
- Weber, W.J., Morris, J.C., 1963. Kinetics of adsorption on carbon from solution. In: *Proceeding of the American Society of Civil Engineers, J. Sanitary Eng. Div.* 89 (SA2), 31–59.
- WHO, 2006. *Chemical Fact Sheets: Fluoride, 1 Guidelines for Drinking Water Quality (Electronic Resource): Incorporation First Addendum, Recommendations*, third ed., vol. 1, WHO, Geneva, pp. 375–377.
- Wu, X., Zhang, Y., Dou, X., Yang, M., 2007. Fluoride removal performance of a novel Fe–Al–Ce trimetal oxide adsorbent. *Chemosphere* 69, 1758–1764.
- Yao, R., Meng, F., Zhang, L., Ma, D., Wang, M., 2009. Defluoridation of water using neodymium-modified chitosan. *J. Hazard. Mater.* 165, 454–460.